Post-Print

N. Zurlo, S. Aghion, C. Amsler, M. Antonello, A. Belov, G. Bonomi, R.S. Brusa, M. Caccia, A. Camper, R. Caravita, F. Castelli, G. Cerchiari, D. Comparat, G. Consolati, A. Demetrio, L. Di Noto, M. Doser, C. Evans, M. Fanì, R. Ferragut, J. Fesel, A. Fontana, S. Gerber, M. Giammarchi, A. Gligorova, F. Guatieri, P. Hackstock, S. Haider, A. Hinterberger, H. Holmestad, A. Kellerbauer, O. Khalidova, D. Krasnický, V. Lagomarsino, P. Lansonneur, P. Lebrun, C. Malbrunot, S. Mariazzi, J. Marton, V.A. Matveev, S.R. Müller, G. Nebbia, P. Nedelec, M. Oberthaler, D. Pagano, L. Penasa, V. Petracek, F. Prelz, M. Prevedelli, B. Rienaecker, J. Robert, O.M. Røhne, A. Rotondi, M. Sacerdoti, H. Sandaker, R. Santoro, L. Smestad, F. Sorrentino, G. Testera, I.C. Tietje, M. Vujanovic, E. Widmann, P. Yzombard, C. Zimmer, J. Zmeskal

Monte-Carlo Simulation of Positronium Laser Excitation and Anti-Hydrogen Formation via Charge Exchange
Hyperfine Interactions, Vol. 240, 18, 2019, p. 1-11
doi:10.1007/s10751-019-1553-3

Noname manuscript No.
(will be inserted by the editor)

Monte-Carlo simulation of positronium laser excitation and anti-hydrogen formation via charge exchange

Nicola Zurlo · Stefano Aghion · Claude Amsler · Massimiliano Antonello · Alexandre Belov · Germano Bonomi · Roberto S. Brusa · Massimo Caccia · Antoine Camper · Ruggero Caravita · Fabrizio Castelli · Giovanni Cerchiari · Daniel Comparat · Giovanni Consolati · Andrea Demetrio · Lea Di Noto · Michael Doser · Craig Evans · Mattia Fanì · Rafael Ferragut · Julian Fesel · Andrea Fontana · Sebastian Gerber · Marco Giammarchi · Angela Gligorova · Francesco Guatieri · Philip Hackstock · Stefan Haider · Alex Hinterberger · Helga Holmestad · Alban Kellerbauer · Olga Khalidova · Daniel Krasnický · Vittorio Lagomarsino · Pierre Lansonneur · Patrice Lebrun · Chloe Malbrunot · Sebastiano Mariazzi · Johann Marton · Victor A. Matveev · Simon R. Müller · Giancarlo Nebbia · Patrick Nedelec · Marcus Oberthaler · Davide Pagano · Luca Penasa · Vojtech Petracek · Francesco Prelz · Marco Prevedelli · Benjamin Rienaecker · Jacques Robert · Ole M. Røhne · Alberto Rotondi · Michele Sacerdoti · Heidi Sandaker · Romualdo Santoro · Lillian Smestad · Fiodor Sorrentino · Gemma Testera · Ingmari C. Tietje · Milena Vujanovic · Eberhard Widmann · Pauline Yzombard · Christian Zimmer · Johann Zmeskal
(AEgIS Collaboration)

Received: date / Accepted: date

N. Zurlo
Department of Civil, Environmental, Architectural Engineering and Mathematics, University of Brescia, Italy
INFN Sezione di Pavia, Pavia, Italy
E-mail: nicola.zurlo@cern.ch
Tel.: 00393496338242

S. Aghion, C. Evans, R. Ferragut
LNESS, Department of Physics, Politecnico di Milano, Como, Italy
INFN Sezione di Milano, Milano, Italy

C. Amsler, A. Gligorova, P. Hackstock, J. Marton, E. Widmann, J. Zmeskal
Stefan Meyer Institute for Subatomic Physics, Vienna, Austria

M. Antonello, M. Caccia, R. Santoro
INFN Sezione di Milano, Milano, Italy
Department of Science, University of Insubria, Como, Italy

A. Belov
Institute for Nuclear Research of the Russian Academy of Sciences, Moscow, Russia

G. Bonomi, D. Pagano
Department of Mechanical and Industrial Engineering, University of Brescia, Brescia, Italy
INFN Sezione di Pavia, Pavia, Italy

R. S. Brusa, F. Guatieri, S. Mariazzi, L. Penasa
Department of Physics, University of Trento, Trento, Italy
TIFPA/INFN Trento, Trento, Italy

A. Camper, R. Caravita, M. Doser, M. Fanì, J. Fesel, S. Gerber, S. Haider, A. Hinterberger, O. Khalidova, C. Malbrunot, B. Rienaecker, I. C. Tietje, M. Vujanovic
Physics Department, CERN, Geneva, Switzerland

F. Castelli
INFN Sezione di Milano, Milano, Italy
Department of Physics “Aldo Pontremoli”, University of Milano, Milano, Italy

G. Cerchiari, A. Kellerbauer, P. Yzombard
Max Planck Institute for Nuclear Physics, Heidelberg, Germany

D. Comparat, J. Robert
Laboratoire Aimé Cotton, Université Paris-Sud, ENS, Université Paris-Saclay, Orsay, France

G. Consolati
Department of Aerospace Science and Technology, Politecnico di Milano, Milano, Italy
INFN Sezione di Milano, Milano, Italy

A. Demetrio, S. R. Müller, M. Oberthaler
Kirchhoff Institute for Physics, Heidelberg University, Heidelberg, Germany

L. Di Noto, V. Lagomarsino, F. Sorrentino
Department of Physics, University of Genova, Genova, Italy
INFN Sezione di Genova, Genova, Italy

A. Fontana
INFN Sezione di Pavia, Pavia, Italy

M. Giammarchi, F. Prelz, M. Sacerdoti
INFN Sezione di Milano, Milano, Italy

H. Holmestad, O. M. Røhne, H. Sandaker
Department of Physics, University of Oslo, Oslo, Norway

D. Krasnický, G. Testera
INFN Sezione di Genova, Genova, Italy

P. Lansonneur, P. Lebrun, P. Nedelec
Institute of Nuclear Physics, CNRS/IN2p3, University of Lyon 1, Villeurbanne, France

V. A. Matveev
Joint Institute for Nuclear Research, Dubna, Russia
Institute for Nuclear Research of the Russian Academy of Science, Moscow, Russia

Abstract The AEgIS experiment aims at producing antihydrogen (and eventually measuring the effects of the Earth gravitational field on it) with a method based on the charge exchange reaction between antiproton and Rydberg positronium. To be precise, antiprotons are delivered by the CERN Antiproton Decelerator (AD) and are trapped in a multi-ring Penning trap, while positronium is produced by a nanoporous silica target and is excited to Rydberg states by means of a two steps laser excitation. New Monte Carlo simulations are presented in this paper in order to investigate the current status of the AEgIS experiment [1] and to interpret the recently collected data [2].

Keywords Positronium · Charge exchange · Anti-hydrogen atoms

PACS 78.70.Bj · 34.80.Lx · 36.10.Dr · 36.10.-k

1 Introduction

Since the first synthesis of cold antihydrogen [3], several experiments in the same field [4–6] have exploited (and substantially improved) the same technique, based on the mixing of positrons and antiprotons clouds interacting via three body recombination, with only one relevant exception [7]. In this work, the feasibility of a different way to antihydrogen production was demonstrated, via antiproton-positronium charge exchange mediated by cesium atoms, along the lines of a method first proposed in a pioneering work published in 1986 [8] and subsequently investigated by other research groups (see e.g. [9–11]).

The AEgIS experiment aims at producing antihydrogen (and eventually measuring the effects of the Earth gravitational field on it) with a similar method, based on the charge exchange reaction between antiproton ($\bar{p}$) and positronium (Ps):

$$\bar{p} + Ps^* \rightarrow \bar{H}^* + e^-$$

G. Nebbia
INFN Sezione di Padova, Padova, Italy

V. Petracek
Czech Technical University, Prague, Czech Republic

M. Prevedelli
University of Bologna, Bologna, Italy

A. Rotondi
Department of Physics, University of Pavia, Pavia, Italy
INFN Sezione di Pavia, Pavia, Italy

L. Smestad
Physics Department, CERN, Geneva, Switzerland
The Research Council of Norway, Lysaker, Norway

C. Zimmer
Physics Department, CERN, Geneva, Switzerland
Max Planck Institute for Nuclear Physics, Heidelberg, Germany
Department of Physics, Heidelberg University, Heidelberg, Germany

where Ps is produced by positrons implantation on a mesoporous silica target and subsequently excited to a Rydberg state (Ps^*) via double step laser excitation [12].

This process can be in principle more efficient than the traditional mixing process, because of the large cross section for Rydberg charge exchange, and has the advantage that the final $\bar{H}$ quantum states can be predicted as a function of the initial Ps^* quantum states, and their distribution is relatively narrow, so that they can be accelerated by electric field gradients. Moreover, antiprotons can be preemptively cooled in order to reduce their transverse velocity and make a collimated beam of antihydrogen (via Stark acceleration technique).

In this paper, we will focus on Monte Carlo simulations designed for the assessment of the Ps laser excitation in the antiproton Penning trap region, and then developed to give an estimation of the antihydrogen production rate.

2 Monte Carlo Simulation

The simulations presented here reflects the current (March 2018) state of the art of the AEgIS experiment, and include:

1. the impingement of the positron bunch on a suitable nanoporous target [14] to produce cold Ps which is emitted into vacuum (a simple model is adopted, supposing that Ps is thermally distributed out of the surface where positrons collide)
2. the Ps excitation in a Rydberg state (Ps^*) by means of two laser pulses with suitable wavelength and duration $1,5-3$ ns [12,13]
3. the formation of cold Rydberg anti-hydrogen $\bar{H}^*$ from a charge exchange reaction between antiprotons and Ps^*

The whole system described here is kept in a 1 T magnetic field (to limit Ps^* self-ionization), where antiprotons are preemptively transferred and stored in a multi-ring Penning trap (after being caught and cooled with electrons in a 5 T magnetic field), see Figure 1.

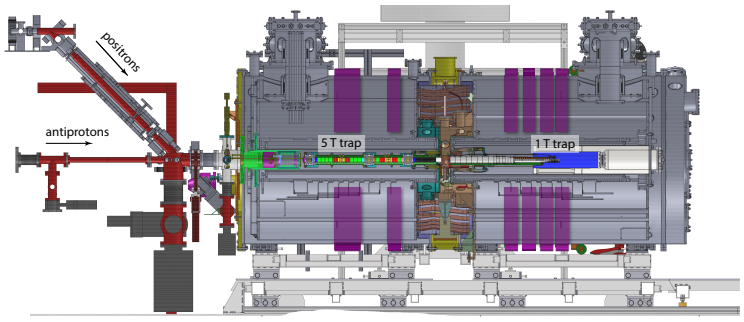

Fig. 1 Drawing of the full AEgIS apparatus. The region discussed in this paper is the so-called 1 T trap. The detectors used to read the signals discussed later in the text are the scintillating slabs (depicted in violet) surrounding the apparatus and read by standard photomultipliers (Philiphs-Photonis XP2020 and Thorn-EMI 9954B).

2.1 Simulation Design

The simulation has been developed using Wolfram Mathematica®[1] version 11.2 and it has been designed to separately deal with the tracking problem (we assume that *Ps* moves along straight lines in a space filled with the CAD model of the region surrounding the target, including the $\bar{p}$-trap electrodes) and with the evolution of each *Ps* along its track (namely the possible laser excitation until the eventual annihilation in flight or on the wall).

In the following, the former will be called "spatial simulation" while the latter will be called "temporal simulation". Since the spatial simulation is much more time consuming than its temporal counterpart (essentially because of the complexity of the involved geometry), the spatial simulation was usually run once for a specific CAD geometry and positron beam setup, then the output was written in a lookup table, and eventually several temporal simulations (with different physical parameters, e.g. laser timing and beam size) were carried out on this basis.

The first goal for our simulation was to assess the presence (and the fraction) of Ps^* and to understand the observed SSPALS spectra[2] which were not clear because of the intricate geometry and the short free path available for *Ps*. But it turned out that the implemented method can be easily modified to incorporate new modules, for example the simulation of $\bar{H}$ production (once included the information about the $\bar{p}$ plasma size and density and a model for charge exchange cross section, like the one reported in [18]).

Spatial simulation The aim of the spatial simulation is to track each *Ps* and measure its maximal free path (independently of its lifetime, see Figure 2), as well as the amount of *Ps* which can reach the $\bar{p}$ plasma.

The spatial simulation of the *Ps* tracks has been performed using the following parameters:

- the measured size of the positron bunch impinging on the target ($\sigma_v \simeq 0.3$ mm, $\sigma_h \simeq 0.1$ mm)
- the measured position of the center of the positron bunch impinging on the target (distance from the trap axis 13 mm, position situated in the vertical plane passing through the trap axis)
- a *Ps* source obtained by the projection of such a beam on the target surface
- a *Ps* emission assumed to be uniformly distributed in a cone of 120° opening angle and axis perpendicular to the target surface.

[1] This particular software was chosen over alternatives (like e.g. Geant 4) because no real passage of particles through matter was involved, most of the phenomena occurred in vacuum, and particle interactions were dominated by only a few physics processes, which needed some *ad hoc* models implemented. On the other hand, with Mathematica we had the advantage of gaining a lot in readibility of the results, being able to easily follow the outcome of each step of the experiment, to quantify the effect of any change in the setup, making it easier the whole optimisation in order to achieve our goal.

[2] Single-Shot Positron Annihilation Lifetime Spectroscopy, a method for detecting and analysing delayed annihilations due to *Ps* succeeding the prompt annihilation burst produced by positrons, in order to gather information about the fraction of *Ps* and its properties. Both kind of annihilations are observed through gamma radiation detected by a fast scintillator, coupled with a rapid photomultiplier and whose signal is recorded by a fast oscilloscope (see [15, 16] for the conception and precise definition of SSPALS, as well as [17] for a recent review on the capability to disentangle also *Ps* laser excitation effects).

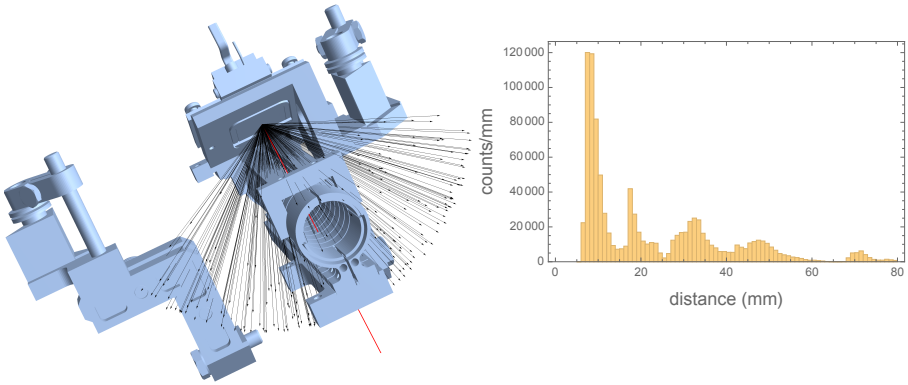

Fig. 2 Left: drawing of the system formed by the nested Penning trap for antiprotons and the *Ps* emitting target, with some example *Ps* tracks depicted by arrows (in red the straight line perpendicular to the target; $\bar{p}$ plasma is not represented inside the trap). Right: histogram of the *Ps* free path (defined as the distance between the Ps track source and its impact point on the surrounding items or walls).

Temporal simulation If the aim of the spatial simulation is to track each *Ps* and measure its free path, the temporal simulation has the goal to reproduce the real *Ps* annihilation signal, and its change in the presence of laser excitation.

Once terminated the spatial simulation, the data about the starting points and the impact points of each track are recorded and passed to the subsequent temporal simulation. In fact, the temporal simulation takes into account all the remaining relevant processes, i.e.:

- the *Ps* velocity distribution, usually a Maxwellian distribution (i.e. a Maxwell-Boltzmann kinetic energy distribution with average $\frac{3}{2}k_BT$, where T is the supposed *Ps* absolute temperature; the measured average velocities are typically $\sim 10^5$ m/s.
- the *Ps* lifetime distribution (exponential with average lifetime $\tau = 142$ ns)
- the temporal spread in the *Ps* emission time (usually 4-6 ns RMS).
- a model for the laser excitation to a Rydberg level taking into account not only the laser beam size and position, but also the saturation fluence [13] and the Doppler effect (that adds a further efficiency depending on the laser bandwidth and on the *Ps* velocity component parallel to the laser direction, $v_{\|}$)

All these data are evaluated to calculate the excitation probability for every *Ps* track; the simulation then creates an event with that probability and, in the presence of excitation, the annihilation is delayed: the "unexcited *Ps*" keeps the original lifetime (and annihilates with this lifetime or on the wall if it is hit beforehand, see Figure 3), otherwise Ps^* gets a new lifetime, again exponentially distributed, but with a much larger average - so that it annihilates almost always on the wall.

In order to reproduce the signal observed in the experimental data by scintillation detectors, which is due to gamma rays not only produced by orhopositronium but also

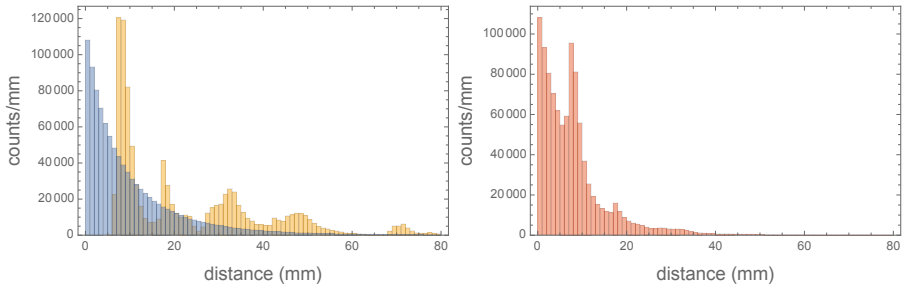

Fig. 3 Left: histogram of the distance traveled by *Ps* on the basis of its exponential lifetime for a Maxwellian velocity distribution at $T = 300$ K (in blue, to be compared with the maximal free path of Figure 2, reported also here for clarity, in yellow). Right: histogram of the overall distance traveled by *Ps*, i.e. the minimum between them. In these conditions, around 22% of the *Ps* annihilate on the wall, and the rest in flight.

by parapositronium and by direct positron annihilations on the target, the simulation takes eventually into account other effects not mentioned in the previous list (like the fraction of prompt annihilations, around 75%, and the detector response function; see Figure 4). From the same figure, it may also be inferred that the difference between the scintillator signals in the presence and in the absence of laser excitation is always more than one order of magnitude smaller than the signal itself, mainly because of the limited laser bandwidth (see also Figure 5) and of the delayed light emission in the scintillator.

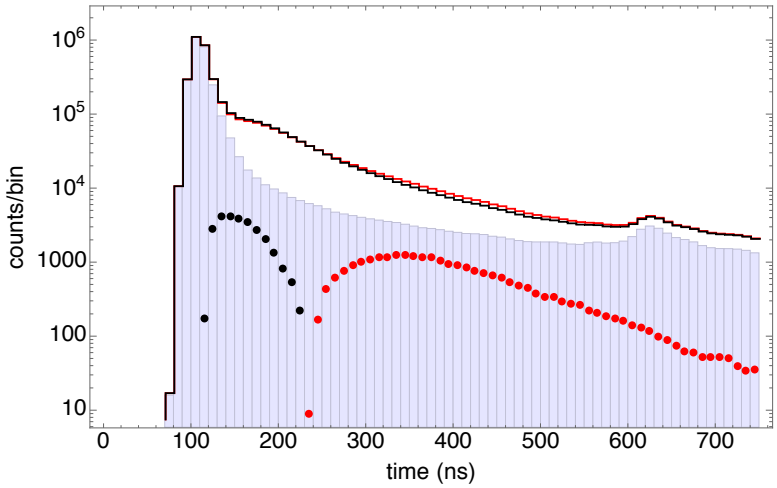

Fig. 4 Detector signal from gamma annihilations expected from the simulation in case of no laser excitation (black line histogram) and in case of laser excitation (red line histogram). The faded blue histogram shows the response function of the detector to the bunch of positrons with prompt annihilation. The black dots measure the difference between the two histograms when there is an excess of annihilations when there is no laser excitation (and only *Ps*), while the red dots measure the difference when there is an excess of annihilations with laser excitation (due to the presence of Ps^*).

2.2 Some relevant simulation results

Although there is no room here for showing most of the results, it is important to mention that the Monte Carlo simulation has been proven to be useful in understanding the effect of the delay of the laser with respect to the *Ps* emission, particularly with the target support installed in 2017 that had a ∼0,5 mm gap between the silica target and the region illuminated by the laser beam. In fact, in this case, the laser delay is a very critical parameter because it strongly selects the *Ps* population that undergoes excitation. In Figure 5 we see the distributions for the velocity parallel to the laser propagation direction (whose changes are dominated by the Doppler effect) as well as the velocity perpendicular to the laser propagation direction for a laser delay of 45 ns, that looks to be the most effective for *Ps* emitted at 300 K by this target. Smaller laser delays are slightly less effective on the number of excited *Ps* but select a population with higher velocity to be excited, and vice-versa (as can be inferred from Figure 6 we see the distributions for the velocity perpendicular to the laser propagation direction for a laser delay of 15 ns and for a laser delay of 85 ns).

After studying the properties of the Ps^* distribution, the same simulation was extended to evaluate the $\bar{H}$ production by interaction of the Ps^* (typically with $n = 16$ in AEgIS) with the antiproton plasma, with a measured size of 4 mm (radially) $\times$ 2 mm (axially), a central density of 25 $\times 10^6$ cm^{-3} (for more details on the techniques used in AEgIS to reach such densitiies, see [19]) and a (roughly estimated)

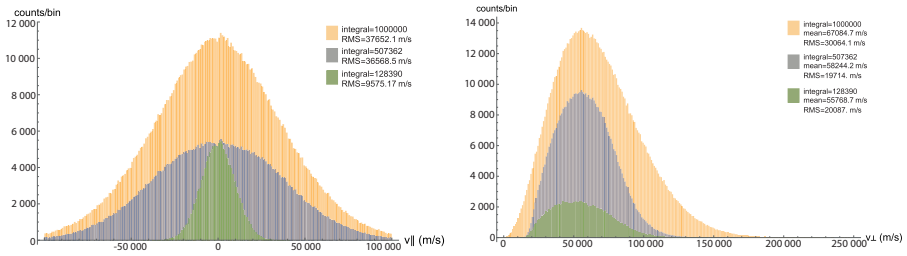

Fig. 5 Velocity distributions for *Ps* emitted from the target (yellow histogram), for *Ps* reached by the laser (grey histogram) and for *Ps* that results excited to Rydberg state (green histogram). Left: distribution for the velocity parallel to the laser ($v_\parallel$). Right: distribution for the velocity perpendicular to the laser ($v_\perp$). The histograms are normalized to the number of effective Ps^* in the simulation. The laser delay is set to 45 ns.

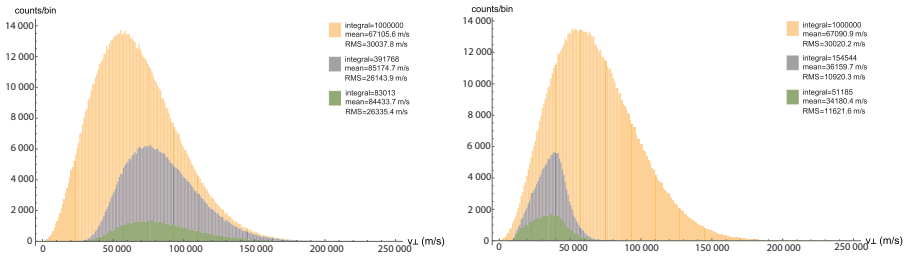

Fig. 6 Distributions for the velocity perpendicular to the laser ($v_\perp$, color codes as in Figure 5). Left: distribution for a laser delay of 15 ns. Right: distribution for a laser delay of 85 ns

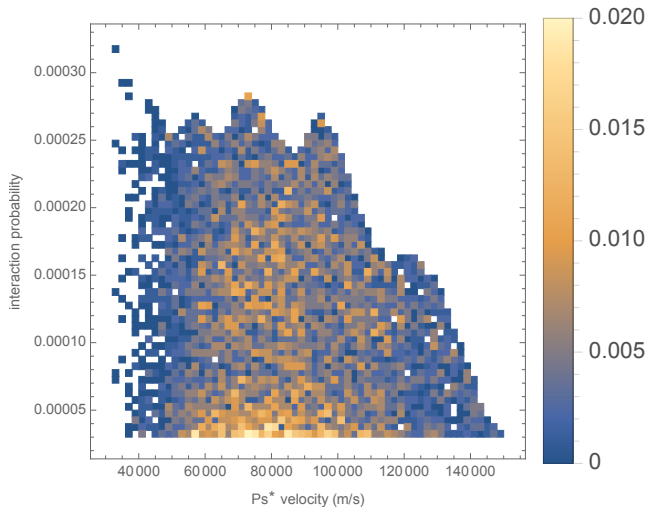

Fig. 7 Joint distribution as a function of the $\bar{H}$ formation probability and of the Ps^* velocity.

temperature of around 1000 K. In order to evaluate the $\bar{H}$ production probability, the cross section given in [18] was used. The average number of produced $\bar{H}$ was estimated to be around 1 per 10^6 Ps emitted by the target. In Figure 7, for example, we see the joint probability distribution as a function of the interaction probability and of the Ps^* velocity: as expected, the highest interaction probability corresponds to low Ps^* velocities, while the main contribution to the $\bar{H}$ production is given by Ps^* with intermediate velocities (which are in larger number).

3 Conclusions

In this work, we have presented some results from a Monte Carlo simulation aimed at a better understanding of the phenomena occurring in the AEgIS experiment, in particular for what concerns the optimisation of the overlap between Ps and the laser beam, the interpretation of the data collected in order to apply the SSPALS method to estimate the fraction of Ps^*, the evaluation of the flux of the Ps^* reaching the antiproton plasma and finally the $\bar{H}$ production.

Moreover, the simulation helped identify some critical points in the design of the target used in 2017 that were subsequently amended.

With the help of new diagnostic tools currently under development in AEgIS, we think it will be a valuable device to put new constraints on some of the poorly known properties of the system we deal with (like e.g. the Ps velocity distribution).

References

1. G. Drobychev et al., Proposal for the AEGIS experiment at the CERN antiproton decelerator (Antimatter Experiment: Gravity, Interferometry, Spectroscopy), CERN-SPSC-2007-017 (2007)

2. M. Doser. et al., Progress report on the AEgIS experiment, CERN-SPSC-2018-005 (2017)
3. M. Amoretti et al., Production and detection of cold antihydrogen atoms, Nature **419** (2002)
4. G. Andresen, et al., Trapped antihydrogen, Nature **468** 673 (2010)
5. G. Gabrielse et al., Trapped antihydrogen in its ground state, Phys. Rev. Lett. **108** 113002 (2012)
6. Y. Enomoto et al., Synthesis of cold antihydrogen in a cusp trap, Phys. Rev. Lett. 105 (24) (2010) 243401
7. C.H. Storry et al., First Laser-Controlled Antihydrogen Production, Phys. Rev. Lett. **93**, 263401 (2004)
8. B.I. Deutch, A.S. Jensen, A. Miranda and G.C. Oades. Proceedings of The First Workshop on Antimatter Physics at Low Energy, 371, FNAL (1986)
9. B.I. Deutch et al., Antihydrogen Production by Positronium-Antiproton Collisions in an Ion Trap, Physica Scripta, Volume 1988, T22
10. E.A. Hessels D.M. Homan and M.J. Cavagnero, Two-stage Rydberg charge exchange: An efficient method for production of antihydrogen, Phys. Rev. A **57** (1998)
11. M. Charlton and J.W. Humberston, Positron Physics, Cambridge University Press, chapter 6 (2000)
12. S. Aghion et al., Laser excitation of the $n = 3$ level of positronium for antihydrogen production, Phys. Rev. A **94**, 012507 (2016)
13. F. Castelli, I. Boscolo, S. Cialdi and M. G. Giammarchi, Efficient positronium laser excitation for antihydrogen production in a magnetic field Phys. Rev. A **78** 052512 (2008)
14. S. Mariazzi P. Bettotti and Roberto S. Brusa Positronium Cooling and Emission in Vacuum from Nanochannels at Cryogenic Temperature, Phys. Rev. Lett. **104** 243401 (2010)
15. D.B. Cassidy, S.H.M. Deng, H.K.M. Tanaka and A.P. Mills Jr., Single shot positron annihilation lifetime spectroscopy. Appl. Phys. Lett. **88**, 194105 (2006).
16. D.B. Cassidy and A.P. Mills Jr., A fast detector for single-shot positron annihilation lifetime spectroscopy, Nucl. Instrum. Meth. A **580**, 1338 (2007)
17. A. Deller, SSPALS: A tool for studying positronium, Nucl. Instrum. Meth. A **922**, 91 (2019).
18. D. Krasnicky, R. Caravita, C. Canali and G. Testera, Cross section for Rydberg antihydrogen production via charge exchange between Rydberg positroniums and antiprotons in a magnetic field, Phys. Rev. A **94**, 022714 (2016)
19. S. Aghion et al., Compression of a mixed antiproton and electron non-neutral plasma to high densities, Eur. Phys. J. D **72**, 76 (2018)